

# On Convex Vector Precoding for Multiuser MIMO Broadcast Channels

Rodrigo de Miguel and Ralf R. Müller, *Senior Member, IEEE*

**Abstract**—We propose different convex alphabet relaxation schemes for vector precoding in MIMO broadcast channels using binary, quaternary and octonary modulation. Expressions are presented for the probability of the different precoding schemes to achieve interference-free communication over singular channels. The energy of transmission is evaluated in the many user limit using the replica method from statistical physics. An alternative channel inversion technique is proposed which makes purely real binary alphabets perform as well as their complex extensions, resulting in reduced complexity in the optimization process. The relevance of the asymptotic analysis is confirmed by finite size simulations.

**Index Terms**—Asymptotic analysis, channel inversion, multiple antennas, multiple-input multiple-output (MIMO) systems, nonlinear vector precoding, random matrices, replica method, R-transform, singular channels, zero-forcing.

## I. INTRODUCTION

**I**N multiple-input/multiple-output (MIMO) channels information is conveyed simultaneously from a group of transmitting antennas to a group of receiving antennas. As these transmissions are not necessarily orthogonal, yet they occur over the same physical medium and bandwidth, crosstalk becomes unavoidable. As a result signal processing needs to be done at the receiver and/or transmitter side of the channel if significant data rates are to be achieved. In the context of low cost receivers with limited processing power and battery life, it might be advantageous to shift most of the signal processing to the transmitter side.

In the case of the MIMO-broadcast channel, depicted in Fig. 1, the receiving antennas are at different locations, which means that they might not jointly process the data they independently receive. The transmitting antennas, however, are collocated and they jointly generate the data streams to be transmitted to each of the single receiving antennas, also referred to as users. One technique which might be employed by the transmitter in order keep the users from doing any signal

Manuscript received October 06, 2008; accepted March 30, 2009. First published June 30, 2009; current version published October 14, 2009. The associate editor coordinating the review of this manuscript and approving it for publication was Dr. Biao Chen. This material is based upon work supported in part by the Research Council of Norway under Grant 171133/V30. This paper was presented in part at the IEEE International Zürich Seminar on Communications, Zürich, Switzerland, 2008 and the IEEE International Symposium on Personal, Indoor and Mobile Radio Communications, Cannes, France, 2008.

The authors are with the Department of Electronics and Telecommunications, The Norwegian University of Science and Technology, 7491 Trondheim, Norway (e-mail: rodrigo@iet.ntnu.no; ralf@iet.ntnu.no).

Color versions of one or more of the figures in this paper are available online at <http://ieeexplore.ieee.org>.

Digital Object Identifier 10.1109/TSP.2009.2026517

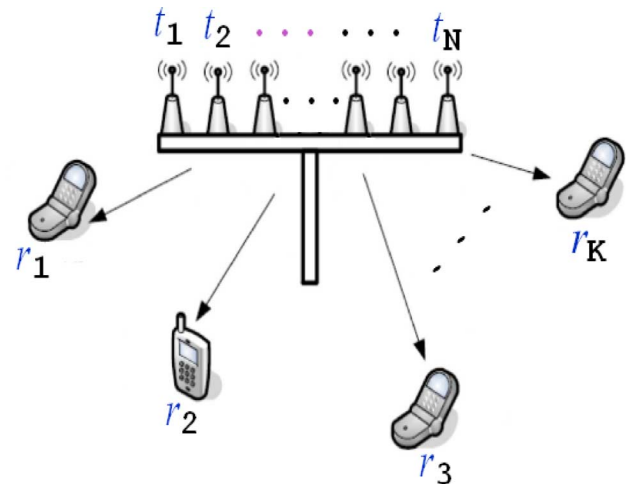


Fig. 1. A MIMO broadcast channel with  $N$  transmitting antennas and  $K$  single-antenna receivers.

processing is channel inversion before transmission (provided that the transmitter has complete channel state information). Unfortunately, plain channel inversion at the transmitter comes at an increased transmission energy cost. One technique which may be used to contain the transmit power while inverting the channel is nonlinear vector precoding (henceforth vector precoding) [1]–[4]. The vector precoding technique, outlined in Section II, consists of extending the input alphabets representing different information states; this permits the search for symbols which draw less energy when transmitted with channel inversion.

In [5] one of the authors proposed *convex precoding*, a new precoding technique not based on lattice extensions of the symbol constellations. The original appeal of this precoding technique was that it allows for convex optimization procedures to find the data vector with the minimum transmitted energy. Later results showed that convex alphabets can be competitive compared to lattice alphabets in terms of mutual information [6], [7]. Additionally, we have recently discovered that convex precoding allows, in principle, for vector precoding in cases where the channel matrix is rank deficient, i.e., when the number of data streams is greater than the number of receive antennas, while creating neither crosstalk nor the need for any particular signal processing at the receiver side [8]. This feature makes convex precoding an attractive candidate for MIMO systems with fewer transmit than receive antennas, or in cases where the MIMO channel exhibits rank deficiencies due to key-hole effects.

A convex relaxation scheme for quaternary phase shift keying (QPSK) constellations was introduced in [5], and the

possibility of overloading was addressed in the large system limit, i.e., when the number of antennas at both ends of the link grows towards infinity. In [8] it was shown that the possibility of overloading was not just an artefact of the large-system analysis. Rigorous mathematical means were employed to show that, with high probability, overloading is possible in finite sized systems as well; this probability was calculated, as a function of the number of antennas, for MIMO channels with arbitrary correlations.

In the present contribution we explore convex precoding for modulation schemes other than QPSK. In particular we explore binary and octonary modulation schemes, for which a suitable choice of a convex relaxed symbol set is not clear. We propose several novel relaxed convex sets and find their corresponding probability to achieve interference-free transmission over finite singular channels. The system performance (in terms of transmitted energy versus uncoded transmission rate) is analyzed in the large system limit by means of the replica method from statistical physics.

Considering binary phase shift keying (BPSK), Schober *et al.* [9] showed that the real part of the matched filter output gives sufficient statistics for multiuser detection on a multiple-access channel. It can be seen as a dual result for precoding on the broadcast channel, that we find in this work that convex relaxations for BPSK can be restricted to the real line without loss in performance. Like in [9], this requires replacing the linear part of the signal processing, i.e., channel inversion, with widely linear processing.

This paper is organized as follows. The vector precoding technique is outlined in Section II. In Section III methods from statistical physics are used to derive the transmitted energy in the many user limit. Sections IV, V, and VI present, respectively, alphabet relaxation schemes for quaternary, binary, and octonary modulation. In Section VII we find the probability of the different relaxation schemes to achieve interference-free transmission. The results are presented in Section VIII. Some technical details, including those of the replica method, are relegated to the Appendices.

## II. VECTOR PRECODING

We consider a narrowband MIMO broadcast channel, which may be represented by the following vector equality:

$$\mathbf{r} = \mathbf{H}\mathbf{t} + \mathbf{n} \quad (1)$$

where  $\mathbf{t}$  is the  $N$ -dimensional input to the channel,  $\mathbf{r}$  is a vector containing the  $K$  received data streams,  $\mathbf{n}$  is a random vector containing additive noise components, and the channel matrix  $\mathbf{H}$  is a complex rectangular matrix which can be written as  $\mathbf{H} = \mathbf{H}_r + j\mathbf{H}_i$ , where  $\mathbf{H}_r$  and  $\mathbf{H}_i$  are real random matrices containing independent and identically distributed (i.i.d.) entries with zero mean and variance  $1/2$ . Without loss of generality we shall consider single antenna users. See Fig. 1.

The transmitted vector  $\mathbf{t}$  is an  $N$ -dimensional linear transformation of the  $K$  information symbols (contained in  $\mathbf{x}$ ) intended for the  $K$  users, thus we might write

$$\mathbf{t} \equiv \mathbf{T}\mathbf{x}. \quad (2)$$

In order to guarantee individual detection by the receivers, the transmitter, who has complete channel state information, might construct  $\mathbf{T}$  such that the information symbols in  $\mathbf{x}$  can be received interference-free (up to additive noise) by a simple diagonal (yet not necessarily linear) operation  $\hat{\Omega}$  on  $\mathbf{r}$ :

$$\hat{\Omega}\mathbf{r} = \mathbf{x} + \hat{\Omega}\mathbf{n}. \quad (3)$$

Using this transmission scheme, the energy per transmitted symbol is

$$K^{-1}\mathbf{t}^\dagger\mathbf{t} = K^{-1}\mathbf{x}^\dagger\mathbf{E}\mathbf{x} \quad (4)$$

where the energy metric  $\mathbf{E}$  is given by

$$\mathbf{E} = \mathbf{T}^\dagger\mathbf{T}. \quad (5)$$

### A. Channel Inversion

The  $K \times K$  matrix  $\mathbf{H}\mathbf{H}^\dagger$  has rank given by  $\min\{N, K\}$ , and its inverse exists only if  $K \leq N$ . A channel is said to be overloaded when there are more receiving users than there are antennas at the transmitter, i.e.,  $K > N$ . In order to allow for the possibility of inverting overloaded channels, the transmitter might employ the generalized channel inversion technique outlined in the following.

When a matrix  $\mathbf{M}$  is Hermitian, as is  $\mathbf{H}\mathbf{H}^\dagger$ , we might write

$$\mathbf{M} = \mathbf{U}\mathbf{\Lambda}\mathbf{U}^\dagger \quad (6)$$

where  $\mathbf{U}$  is a unitary matrix and  $\mathbf{\Lambda} \equiv \text{diag}(\lambda_1, \lambda_2, \dots, \lambda_K)$  is a diagonal matrix containing the  $K$  eigenvalues of  $\mathbf{M}$ . We might then define the pseudoinverse of  $\mathbf{M}$  as

$$\mathbf{M}^{-1} \equiv \mathbf{U}\mathbf{\Lambda}^{-1}\mathbf{U}^\dagger \quad (7)$$

where

$$\mathbf{\Lambda}^{-1} \equiv \lim_{\epsilon \rightarrow 0} \text{diag} \left( \frac{1 - \delta_{\lambda_1, 0}}{\lambda_1 + \epsilon}, \frac{1 - \delta_{\lambda_2, 0}}{\lambda_2 + \epsilon}, \dots, \frac{1 - \delta_{\lambda_K, 0}}{\lambda_K + \epsilon} \right) \quad (8)$$

and  $\delta_{i,j}$  is the Kronecker delta.

1) *Complex Symbol Mapping*: If the symbols used to map the data are complex, i.e.,  $\mathbf{x} \in \mathbb{C}^K$ , and the  $K$ -dimensional complex data vector  $\mathbf{x}$  lies in the  $\min\{N, K\}$ -dimensional space spanned by  $\mathbf{H}\mathbf{H}^\dagger$ , then the matrix  $\mathbf{T}$  and the diagonal operator  $\hat{\Omega}$  can be constructed as follows:

$$\mathbf{T} \rightarrow \mathbf{T}_c \equiv \frac{\mathbf{H}^\dagger}{\sqrt{N}} \left( \frac{\mathbf{H}\mathbf{H}^\dagger}{N} \right)^{-1} \quad (9)$$

$$\hat{\Omega} \rightarrow \hat{\Omega}_c \equiv \frac{1}{\sqrt{N}}\mathbf{I}. \quad (10)$$

Then the transmitted energy per symbol is given by

$$K^{-1}\mathbf{t}^\dagger\mathbf{t} = K^{-1}\mathbf{x}^\dagger\mathbf{E}_c\mathbf{x} \quad (11)$$

where

$$\mathbf{E}_c \equiv \mathbf{T}_c^\dagger\mathbf{T}_c = \left( \frac{\mathbf{H}\mathbf{H}^\dagger}{N} \right)^{-1}. \quad (12)$$

TABLE I  
AVERAGE TRANSMIT POWER ENHANCEMENT IN dB FOR CONVEX [5]  
AND LATTICE-BASED [3], [4] VECTOR PRECODED QPSK WITH  $N = 8$   
TRANSMIT ANTENNAS AND  $K$  USERS IN i.i.d. RAYLEIGH FADING

Regularization		$K = 2$	$K = 3$	$K = 4$	$K = 5$	$K = 6$	$K = 7$	$K = 8$
$\gamma = 0$	Convex	1.2	2.0	2.8	3.9	4.8	6.0	8.0
	Lattice	1.2	1.8	2.2	2.6	3.1	3.8	5.0
	difference	0.0	0.2	0.7	1.3	1.7	2.2	3.0
$\gamma = 0.1$	Convex	0.5	1.1	1.7	2.1	2.8	3.3	4.0
	Lattice	0.5	1.0	1.3	1.6	1.9	2.2	2.4
	difference	0.0	0.1	0.4	0.5	0.9	1.1	1.6
$\gamma = 0.5$	Convex	-1.3	-1.0	-0.9	-0.6	-0.4	-0.2	-0.1
	Lattice	-1.3	-1.1	-0.9	-0.7	-0.5	-0.4	-0.3
	difference	0.0	0.0	0.0	0.1	0.1	0.1	0.2

2) *Real Symbol Mapping*: If, on the other hand, only purely real symbols are used to map the data for the  $K$  users, i.e.,  $\mathbf{x} \in \mathbb{R}^K$ , then, as long as the real vectors  $\mathbf{x}$  lie in the span of  $\Re(\mathbf{H}\mathbf{H}^\dagger)$ , the matrix  $\mathbf{T} \rightarrow \mathbf{T}_{\mathcal{R}} = \mathbf{T}_r + \mathbf{j}\mathbf{T}_i$  and the diagonal operator  $\hat{\Omega}$  might be constructed as follows:

$$\begin{bmatrix} \mathbf{T}_r \\ \mathbf{T}_i \end{bmatrix} \equiv \frac{1}{\sqrt{N}} \begin{bmatrix} \mathbf{H}_r^\top \\ -\mathbf{H}_i^\top \end{bmatrix} \left\{ \Re \left( \frac{\mathbf{H}\mathbf{H}^\dagger}{N} \right) \right\}^{-1} \quad (13)$$

$$\hat{\Omega} \rightarrow \hat{\Omega}_{\mathcal{R}} \equiv \frac{1}{\sqrt{N}} \Re \quad (14)$$

where  $\Re$  is the *real-part* operator. Under this transmission scheme, the transmitted energy per symbol is given by

$$K^{-1} \mathbf{t}^\dagger \mathbf{t} = K^{-1} \mathbf{x}^\dagger \mathbf{E}_{\mathcal{R}} \mathbf{x} \quad (15)$$

where

$$\mathbf{E}_{\mathcal{R}} \equiv \mathbf{T}_{\mathcal{R}}^\dagger \mathbf{T}_{\mathcal{R}} = \left\{ \Re \left( \frac{\mathbf{H}\mathbf{H}^\dagger}{N} \right) \right\}^{-1}. \quad (16)$$

It is important to note that, as opposed to (12), the matrix whose pseudoinverse is taken in (16) becomes rank deficient only if  $K > 2N$ .

### B. Channel Regularization

Channel inversion allows for interference-free reception at the expense of enhanced transmit power. Allowing for moderate interference, the transmit power enhancement can be reduced by means of channel regularization [4], [10]–[12], i.e., one inverts the matrix  $\mathbf{H}\mathbf{H}^\dagger + \gamma\mathbf{I}$  rather than  $\mathbf{H}\mathbf{H}^\dagger$ . The free parameter  $\gamma$  controls the trade-off between power enhancement and residual interference.

The focus of this work is to contain power enhancement by means of nonlinear methods. These methods work together with both channel inversion and channel regularization. Channel inversion, i.e., channel regularization with  $\gamma = 0$ , is the worst case for our proposed method when compared to lattice precoding, as shown in Table I. Channel inversion is also easier to treat analytically. Having in mind that convex precoding will be even

more competitive for  $\gamma > 0$ , we restrict ourselves in this work to show the benefits of convex precoding for channel inversion.

### C. Minimizing the Transmitted Energy

Although channel inversion by the transmitter keeps the users from having to process any interference, it might come at the cost of a high transmission energy. The goal of the vector precoding technique is minimizing the cost of the channel inversion process, i.e., minimizing (4). For this purpose, it is agreed between the transmitter and the users that, although there must be a minimum distance between any two symbols representing different information states, each state might be represented by more than one symbol. This gives the transmitter greater freedom to construct the information vector  $\mathbf{x}$  with symbols which faithfully represent the intended information, yet they are chosen so as to minimize (4).

The information which the transmitter intends for user  $k$  is the state  $s_k$ . The symbols which might represent the state  $s_k$  are those contained in the set  $\mathcal{A}_{s_k}$ . Then the  $K$ -dimensional vector  $\mathbf{x}$  can be constructed with components  $\{x_1 \in \mathcal{A}_{s_1}, \dots, x_K \in \mathcal{A}_{s_K}\}$ , or, in short  $\mathbf{x} \in \mathcal{A}$ , where  $\mathcal{A} = \mathcal{A}_{s_1} \times \mathcal{A}_{s_2} \times \dots \times \mathcal{A}_{s_K}$ . The transmitter chooses the symbol representation in  $\mathcal{A}$  which can be transmitted free of interference drawing the least energy, i.e.,

$$\mathbf{x} \equiv \arg \min_{\mathbf{x} \in \mathcal{A} \cap \mathcal{S}} K^{-1} \mathbf{x}^\dagger \mathbf{E} \mathbf{x} \quad (17)$$

where  $\mathcal{S}$  denotes the span of  $\mathbf{E}^{-1}$ .

If the symbol alphabets are discrete, the complexity of (17) is exponential in  $K$  [13]. However, if the alphabets representing the different information states are convex, then efficient algorithms might be used to find the optimal  $\mathbf{x}$  [14]. In Sections V, IV, and VI we introduce different convex alphabet relaxation schemes for transmitting 1, 2, or 3 uncoded bits to each user.

## III. THE TRANSMITTED ENERGY: A THERMODYNAMIC APPROXIMATION

The precoding strategy presented in Section II-A is known as standard zero-forcing (SZF) and its goal is to minimize the transmitted energy whilst achieving interference-free and individual reception by the users. A sensible alternative strategy is to minimize the minimum mean-squared-error (MMSE) via channel regularization, see Section II-B. The analysis which follows could very well be done for MMSE precoding; this would, however, require an elaborate analysis of the asymptotics of the inverse regularized matrix ([15, App. 2]) and it would make the results dependent on the regularization parameter. Since SZF and MMSE precoding become essentially identical at high signal-to-noise ratios (SNR) and our goal in this contribution is not to find the optimum linear processing, but instead to compare different relaxations and constellation sets, we choose a high SNR point and let SZF capture the essence of our analysis.

In this section the expression for the transmitted energy per symbol using SZF precoding is presented. First, one might note

that, irrespective of the precoding strategy used, the transmitted energy per symbol  $\mathcal{E}$  might be written as

$$\begin{aligned}\mathcal{E} &\equiv \min_{\mathbf{x} \in \mathcal{A} \cap \mathcal{S}} K^{-1} \mathbf{x}^\dagger \mathbf{E} \mathbf{x} \\ &= - \lim_{\beta \rightarrow \infty} \beta^{-1} K^{-1} \ln \sum_{\mathbf{x} \in \mathcal{A} \cap \mathcal{S}} e^{-\beta \mathbf{x}^\dagger \mathbf{E} \mathbf{x}}.\end{aligned}\quad (18)$$

The argument of the  $\beta$  limit in (18) has the same form as the expression for the *Helmholtz free energy* of a thermodynamic ( $K \rightarrow \infty$ ) system with temperature  $1/\beta$  which can exist in the states  $\mathbf{x} \in \mathcal{A} \cap \mathcal{S}$  and whose energy is dictated by the interaction matrix  $\mathbf{E}$  [16]. In the following we take advantage of this fact by taking a thermodynamic approximation, i.e., we always assume that  $K$  and  $N$  are infinitely large, yet they have a finite ratio  $\alpha = K/N$ . This approximation allows us to make use of mathematical tools imported from the statistical physics literature.

Using the replica method of statistical mechanics and assuming *replica symmetry*, we show in Appendix A that the energy per transmitted symbol (18) is fully determined by the eigendistribution of  $\mathbf{E}$  (which is fully determined by the statistics of  $\mathbf{H}$ ), and the information symbol alphabets, as follows:

$$\mathcal{E} = \frac{\tau}{2} q \frac{d}{d\chi} \chi R_{\mathbf{E}}(-\chi) \quad (19)$$

where  $R_{\mathbf{E}}(\cdot)$ , known as the R-transform of the random matrix  $\mathbf{E}$ , is a function which fully describes the eigenspectrum of  $\mathbf{E}$  (see Appendix B). The parameter  $\tau$  equals 1 when  $\mathbf{E}$  has purely real entries and it equals 2 if the entries are complex.<sup>1</sup> The parameters  $q$  and  $\chi$ , defined as  $q + \beta^{-1}\chi \equiv 2\mathbf{x}^\dagger \mathbf{x} / \tau K$  for  $\mathbf{x}$  given by (17), are given by the following pair of coupled self-consistent equations:

$$q = \frac{2}{\tau} \sum_i P_i \int_{\mathbb{C}} \left| \arg \min_{\xi \in \mathcal{A}_i} \left| \frac{\sqrt{q R'_{\mathbf{E}}(-\chi)}}{R_{\mathbf{E}}(-\chi)} - \frac{\xi}{z} \right| \right|^2 Dz \quad (20)$$

$$\chi = \frac{2}{\tau} \sum_i \frac{P_i}{\sqrt{q R'_{\mathbf{E}}(-\chi)}} \Re \int_{\mathbb{C}} \arg \min_{\xi \in \mathcal{A}_i} \left| \frac{\sqrt{q R'_{\mathbf{E}}(-\chi)}}{R_{\mathbf{E}}(-\chi)} - \frac{\xi}{z} \right| z^* Dz \quad (21)$$

where the index  $i$  denotes the different information states, each of which can be represented by elements in the set  $\mathcal{A}_i$  and occurs in the components of  $\mathbf{x}$  with probability  $P_i$ . The expression  $R'_{\mathbf{E}}(-\chi)$  denotes the first derivative of  $R_{\mathbf{E}}(t)$  evaluated at  $t = -\chi$ . And  $Dz \equiv (e^{-|z|^2})/(\pi) dz$ .

Equations (19)–(21) allow us to find the value of (18) for any unitarily invariant Hermitian random matrix  $\mathbf{E}$  with a converging eigenvalue distribution. As we shall show in Appendix B, for the special case of the SZF matrices  $\mathbf{E} = \mathbf{E}_{\mathcal{C}}$  and  $\mathbf{E} = \mathbf{E}_{\mathcal{R}}$  defined in Section II the energy (19) may be written as

$$\mathcal{E} = \frac{q R'_{\mathbf{E}}(-\chi)}{\alpha R_{\mathbf{E}}^2(-\chi)} \quad (22)$$

<sup>1</sup>The derivation for the special case of  $\tau = 2$  may be found in [5].

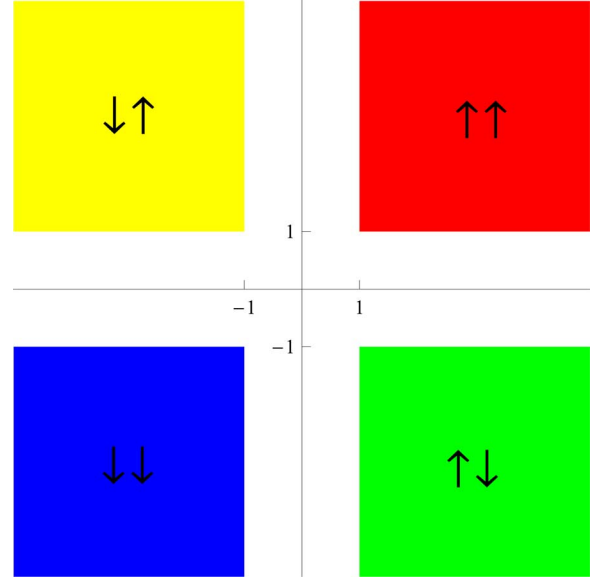


Fig. 2. Quaternary convex relaxation.

and its value reduces to the solution of a single parameter ( $\alpha$ ) self-consistent equation:

$$\mathcal{E} = \frac{\sum_i P_i \int_{\mathbb{C}} \left| \arg \min_{\xi \in \mathcal{A}_i} |z\sqrt{\alpha\mathcal{E}} - \xi| \right|^2 Dz}{1 - \frac{\alpha\tau}{2} + 2\sqrt{\frac{\alpha}{\mathcal{E}}} \sum_i P_i \Re \int_{\mathbb{C}} \arg \min_{\xi \in \mathcal{A}_i} |z\sqrt{\alpha\mathcal{E}} - \xi| z^* Dz}. \quad (23)$$

An important assumption, known as the *replica symmetry ansatz* [17], was made in the derivation of (19)–(23). This assumption has been successfully applied to problems in wireless communications (see, e.g., [18]–[21]) and coding theory (see e.g., [22] and [23]). And, as we shall see in Section VIII, replica symmetry mimics finite size results for the convex alphabets proposed in this work. One should be warned, however, that although replica symmetry yields asymptotically accurate results for convex alphabets, it fails to produce accurate results for alphabets relaxed onto a superlattice. For a recent and novel analysis of lattice alphabets based on replica symmetry breaking the reader is referred to [6] and [7]. For a thorough discussion of replica symmetry, the reader is referred to [24] and [25].

#### IV. CONVEX ALPHABET RELAXATION FOR QPSK

In [5] they considered a source of information consisting of four equiprobable states:  $\uparrow\uparrow, \uparrow\downarrow, \downarrow\downarrow$  and  $\downarrow\uparrow$  and relaxed the standard QPSK alphabets  $\mathcal{A}_{\uparrow\uparrow} = \{1 + j\}, \mathcal{A}_{\uparrow\downarrow} = \{1 - j\}, \mathcal{A}_{\downarrow\downarrow} = \{-1 - j\}, \mathcal{A}_{\downarrow\uparrow} = \{-1 + j\}$  onto the regions shown in Fig. 2. When optimization is independently carried out on the real and imaginary dimensions the energy per transmitted symbol (23) using this alphabet relaxation reduces to

$$\mathcal{E} = \frac{2 + \sqrt{\frac{\alpha\mathcal{E}}{\pi}} e^{-\frac{1}{\alpha\mathcal{E}}} + \{\alpha\mathcal{E} - 2\} Q(\sqrt{2/\alpha\mathcal{E}}) + \alpha\mathcal{E}}{2 + 2\alpha Q(\sqrt{2/\alpha\mathcal{E}})}. \quad (24)$$

The possibility for overloading transmission using this alphabet relaxation was addressed in the asymptotic limit in [5] and for systems of arbitrary size in [8]. In the present work we

shall compare this modulation/relaxation scheme with the binary and octonary schemes we introduce in the following two sections.

## V. CONVEX ALPHABET RELAXATION FOR BINARY PHASE SHIFT KEYING

We consider a source of information consisting of two equiprobable states:  $\uparrow$  and  $\downarrow$ . When no vector precoding is employed the entries in  $\mathbf{x}$  are usually selected from the unit BPSK alphabets  $\mathcal{A}_\uparrow = \{+1\}$  and  $\mathcal{A}_\downarrow = \{-1\}$ . So long as the minimum distance between two points representing different information states is preserved, points might be added to these sets with the aim of reducing the transmitted energy.

In this section we propose two different convex alphabet extension schemes. While one of these alphabets is purely real, the other allows for complex symbols to map the information states. As outlined in Section II, when the symbols used to map the information states are purely real then we might use two different channel inversion schemes. While one of them results in the energy metric (12), which has complex entries, the other one yields the metric (16), whose entries are purely real. The parameter  $\tau$ , remember from Section III, equals 1 when the energy metric  $\mathbf{E}$  contains purely real entries, or 2 when its entries are generally complex. Therefore, when the alphabet under consideration contains complex entries we will automatically set  $\tau = 2$ , whereas for a purely real alphabet it can take any of both values, depending on the channel inversion technique to be employed.

### A. Binary Real Convex Relaxation

A trivial way to relax BPSK onto the real line is as follows:

$$\mathcal{A}_\uparrow = -\mathcal{A}_\downarrow = \{\xi \text{ s.t. } \xi \geq 1\}. \quad (25)$$

This relaxed alphabet, shown in Fig. 3, yields, after (23), the following expression for the energy per transmitted symbol:

$$\mathcal{E} = \frac{2 + \sqrt{\frac{\alpha\mathcal{E}}{\pi}} e^{-\frac{1}{\alpha\mathcal{E}}} + \{\alpha\mathcal{E} - 2\}Q(\sqrt{2/\alpha\mathcal{E}})}{2 - \tau\alpha + 2\alpha Q(\sqrt{2/\alpha\mathcal{E}})} \quad (26)$$

where the function  $Q(\cdot)$  is defined as

$$Q(\sigma) \equiv \frac{1}{\sqrt{2\pi}} \int_\sigma^\infty e^{-\frac{t^2}{2}} dt. \quad (27)$$

### B. Binary Complex Convex Relaxation

The real relaxation space introduced in Section V-A might be further extended onto the complex plane as follows:

$$\mathcal{A}_\uparrow = -\mathcal{A}_\downarrow = \{\xi \in \mathbb{C} \text{ s.t. } \Re\xi \geq 1\}. \quad (28)$$

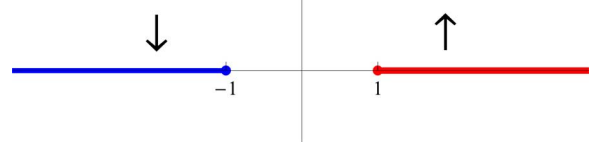


Fig. 3. Binary real convex relaxation.

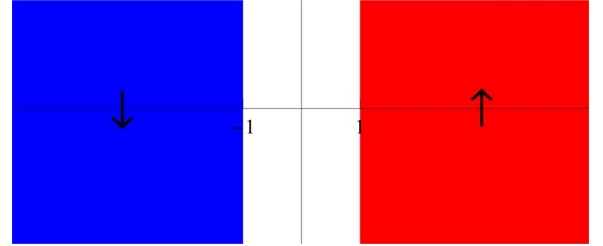


Fig. 4. Binary complex convex relaxation.

As the information states are now mapped onto complex symbols, we might only use the channel inversion scheme resulting in the energy metric (12), which has complex entries. Therefore, the parameter  $\tau$  will now be equal to 2. Under this precoding scheme, shown in Fig. 4, the energy per transmitted symbol reduces, again, to (24). Notice that, when  $\tau = 1$ , (26) reduces to (24) as well.

## VI. CONVEX ALPHABET RELAXATION FOR OCTONARY MODULATION

In this section we consider a source of information consisting of eight equiprobable states,  $\uparrow\uparrow\uparrow, \uparrow\uparrow\downarrow, \uparrow\downarrow\downarrow, \uparrow\downarrow\uparrow, \downarrow\downarrow\uparrow, \downarrow\downarrow\downarrow, \downarrow\uparrow\uparrow$ , and we propose three novel alphabet relaxations for complex octonary modulation.

### A. Fully Symmetric Octonary Relaxation

An octonary phase shift keying (8PSK) constellation typically consists of one-point alphabets given by  $\mathcal{A}_{\uparrow\uparrow\uparrow} = \{1 + \sqrt{2} + j\}$ ,  $\mathcal{A}_{\uparrow\uparrow\downarrow} = \{1 + \sqrt{2} - j\}$ ,  $\mathcal{A}_{\uparrow\downarrow\downarrow} = \{1 - (1 + \sqrt{2})j\}$ ,  $\mathcal{A}_{\uparrow\downarrow\uparrow} = \{-1 - (1 + \sqrt{2})j\}$ ,  $\mathcal{A}_{\downarrow\downarrow\uparrow} = \{-1 - \sqrt{2} - j\}$ ,  $\mathcal{A}_{\downarrow\downarrow\downarrow} = \{-1 - \sqrt{2} + j\}$ ,  $\mathcal{A}_{\downarrow\uparrow\uparrow} = \{-1 + (1 + \sqrt{2})j\}$  and  $\mathcal{A}_{\uparrow\uparrow\uparrow} = \{1 + (1 + \sqrt{2})j\}$ . In order to contain the transmitted energy this alphabet might be symmetrically extended over the complex plane as shown in Fig. 5. These relaxed symbol sets preserve the minimum distance between any two symbols representing different states, and they are given by

$$\begin{aligned} \mathcal{A}_{\uparrow\uparrow\uparrow} &= -\mathcal{A}_{\downarrow\downarrow\downarrow} \\ &= \{\xi \text{ s.t. } \Im\xi \geq 1 \ \& \ \Re\xi \geq \Im\xi + \sqrt{2}\} \\ \mathcal{A}_{\uparrow\uparrow\downarrow} &= -\mathcal{A}_{\downarrow\downarrow\uparrow} \\ &= \{\xi \text{ s.t. } \Im\xi \leq -1 \ \& \ \Re\xi \geq -\Im\xi + \sqrt{2}\} \\ \mathcal{A}_{\uparrow\downarrow\downarrow} &= -\mathcal{A}_{\downarrow\uparrow\uparrow} \\ &= \{\xi \text{ s.t. } \Re\xi \geq 1 \ \& \ \Im\xi \leq -\Re\xi - \sqrt{2}\} \\ \mathcal{A}_{\uparrow\downarrow\uparrow} &= -\mathcal{A}_{\downarrow\uparrow\downarrow} \\ &= \{\xi \text{ s.t. } \Re\xi \leq -1 \ \& \ \Im\xi \leq \Re\xi - \sqrt{2}\} \end{aligned} \quad (29)$$

Under this precoding scheme the energy per symbol (23) reduces to (30), shown at the bottom of the page, where

$$F_1(\mathcal{E}; \alpha) \equiv \frac{1}{8} \sqrt{\frac{\alpha\mathcal{E}}{\pi}} e^{-\frac{1}{\alpha\mathcal{E}}} Q\left(\frac{2+\sqrt{2}}{\sqrt{\alpha\mathcal{E}}}\right) \quad (31)$$

$$F_2(\mathcal{E}; \alpha) \equiv \frac{(1+\sqrt{2})}{8} \sqrt{\frac{\alpha\mathcal{E}}{\pi}} e^{-\frac{3+2\sqrt{2}}{\alpha\mathcal{E}}} Q\left(\frac{-\sqrt{2}}{\sqrt{\alpha\mathcal{E}}}\right) \quad (32)$$

$$F_3(\mathcal{E}; \alpha) \equiv Q\left(\frac{-\sqrt{2}}{\sqrt{\alpha\mathcal{E}}}\right) Q\left(\frac{2+\sqrt{2}}{\sqrt{\alpha\mathcal{E}}}\right) \quad (33)$$

$$I_1(\mathcal{E}; \alpha) \equiv \int_{\frac{1}{\sqrt{\alpha\mathcal{E}}} }^{\infty} ((1+2x^2)\alpha\mathcal{E} - 4) \times Q\left(\frac{2}{\sqrt{\alpha\mathcal{E}}} + \sqrt{2}x\right) \frac{e^{-x^2}}{4\sqrt{\pi}} dx \quad (34)$$

$$I_2(\mathcal{E}; \alpha) \equiv \int_{\frac{1}{\sqrt{\alpha\mathcal{E}}} }^{\infty} ((1+2x^2)\alpha\mathcal{E} - 12 - 8\sqrt{2}) \times Q\left(\frac{2+2\sqrt{2}}{\sqrt{\alpha\mathcal{E}}} - \sqrt{2}x\right) \frac{e^{-x^2}}{4\sqrt{\pi}} dx \quad (35)$$

$$I_3(\mathcal{E}; \alpha) \equiv \int_{\frac{1}{\sqrt{\alpha\mathcal{E}}} }^{\infty} (1+2x^2) \left( Q\left(\frac{2}{\sqrt{\alpha\mathcal{E}}} + \sqrt{2}x\right) + Q\left(\frac{2+2\sqrt{2}}{\sqrt{\alpha\mathcal{E}}} - \sqrt{2}x\right) \right) \frac{e^{-x^2}}{2\sqrt{\pi}} dx. \quad (36)$$

### B. Octonary Stellar Relaxation

We propose an octonary constellation whose original one-point alphabets are given by  $\mathcal{A}_{\uparrow\uparrow\uparrow} = \{2+2j\}$ ,  $\mathcal{A}_{\uparrow\uparrow\downarrow} = \{\sqrt{2}\}$ ,  $\mathcal{A}_{\uparrow\downarrow\downarrow} = \{2-2j\}$ ,  $\mathcal{A}_{\uparrow\downarrow\uparrow} = \{-\sqrt{2}j\}$ ,  $\mathcal{A}_{\downarrow\downarrow\uparrow} = \{-2-2j\}$ ,  $\mathcal{A}_{\downarrow\downarrow\downarrow} = \{-\sqrt{2}\}$ ,  $\mathcal{A}_{\downarrow\uparrow\downarrow} = \{-2+2j\}$  and  $\mathcal{A}_{\downarrow\uparrow\uparrow} = \{\sqrt{2}j\}$ . In order to contain the transmission energy while preserving the minimum distance between any two symbols representing different information states, this alphabet is relaxed as shown in Fig. 6. The extended symbol sets are given by

$$\begin{aligned} \mathcal{A}_{\uparrow\uparrow\uparrow} = -\mathcal{A}_{\downarrow\downarrow\downarrow} &= \{\xi \text{ s.t. } \Re\xi \geq 2 \ \& \ \Im\xi \geq 2\} \\ \mathcal{A}_{\uparrow\uparrow\downarrow} = -\mathcal{A}_{\downarrow\downarrow\uparrow} &= \{\xi \text{ s.t. } \Re\xi \geq \sqrt{2} \ \& \ \Im\xi = 0\} \\ \mathcal{A}_{\uparrow\downarrow\downarrow} = -\mathcal{A}_{\downarrow\uparrow\uparrow} &= \{\xi \text{ s.t. } \Re\xi \geq 2 \ \& \ \Im\xi \leq -2\} \\ \mathcal{A}_{\uparrow\downarrow\uparrow} = -\mathcal{A}_{\downarrow\uparrow\downarrow} &= \{\xi \text{ s.t. } \Re\xi = 0 \ \& \ \Im\xi \leq -\sqrt{2}\} \end{aligned} \quad (37)$$

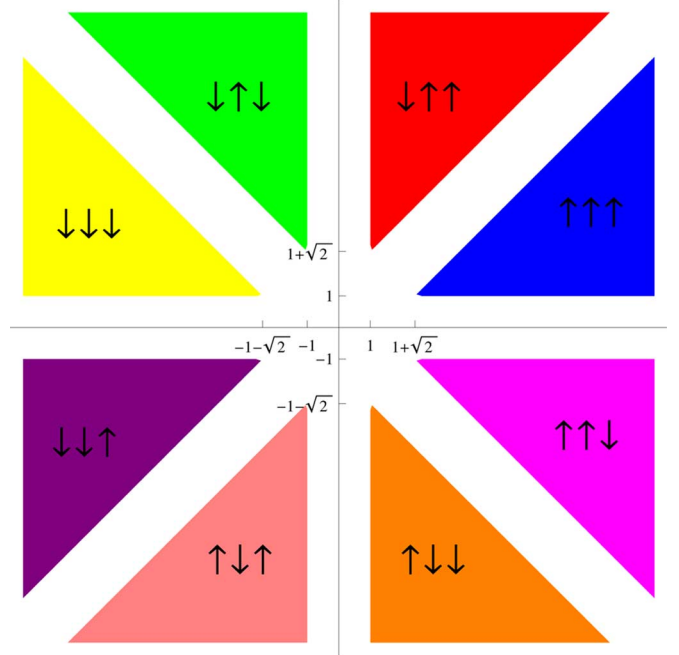


Fig. 5. Fully symmetric octonary relaxation.

and the energy (23) becomes (38), shown at the bottom of the page.

### C. Octonary Triangular Relaxation

An alternative octonary constellation is proposed with unperturbed one-point alphabets given by  $\mathcal{A}_{\uparrow\uparrow\uparrow} = \{2+\sqrt{3}j\}$ ,  $\mathcal{A}_{\uparrow\uparrow\downarrow} = \{1\}$ ,  $\mathcal{A}_{\uparrow\downarrow\downarrow} = \{2-\sqrt{3}j\}$ ,  $\mathcal{A}_{\uparrow\downarrow\uparrow} = \{-\sqrt{3}j\}$ ,  $\mathcal{A}_{\downarrow\downarrow\uparrow} = \{-2-\sqrt{3}j\}$ ,  $\mathcal{A}_{\downarrow\downarrow\downarrow} = \{-1\}$ ,  $\mathcal{A}_{\downarrow\uparrow\downarrow} = \{-2+\sqrt{3}j\}$  and  $\mathcal{A}_{\downarrow\uparrow\uparrow} = \{\sqrt{3}j\}$ . In order to contain the transmission energy and preserve the minimum distance properties of this triangular constellation, only six of the eight points are allowed to relax as shown in Fig. 7. The fact that the two innermost points of the constellation do not undergo any relaxation makes this convex precoding scheme easier to implement. The relaxed symbol sets are given by

$$\begin{aligned} \mathcal{A}_{\uparrow\uparrow\uparrow} = -\mathcal{A}_{\downarrow\downarrow\downarrow} &= \{\xi \text{ s.t. } \Re\xi \geq 2 \ \& \ \Im\xi \geq \sqrt{3}\} \\ \mathcal{A}_{\uparrow\uparrow\downarrow} = -\mathcal{A}_{\downarrow\downarrow\uparrow} &= \{1\} \\ \mathcal{A}_{\uparrow\downarrow\downarrow} = -\mathcal{A}_{\downarrow\uparrow\uparrow} &= \{\xi \text{ s.t. } \Re\xi \geq 2 \ \& \ \Im\xi \leq -\sqrt{3}\} \\ \mathcal{A}_{\uparrow\downarrow\uparrow} = -\mathcal{A}_{\downarrow\uparrow\downarrow} &= \{\xi \text{ s.t. } \Re\xi = 0 \ \& \ \Im\xi \leq -\sqrt{3}\} \end{aligned} \quad (39)$$

$$\mathcal{E} = \frac{3F_1(\mathcal{E}; \alpha) + 7F_2(\mathcal{E}; \alpha) + \frac{1}{2}(\alpha\mathcal{E} - 4\sqrt{2} - 6)F_3(\mathcal{E}; \alpha) + I_1(\mathcal{E}; \alpha) + I_2(\mathcal{E}; \alpha)}{1 - \alpha - \frac{10}{\mathcal{E}}F_1(\mathcal{E}; \alpha) - \frac{2}{\mathcal{E}}F_2(\mathcal{E}; \alpha) + \alpha F_3(\mathcal{E}; \alpha) + \alpha I_3(\mathcal{E}; \alpha)} \quad (30)$$

$$\mathcal{E} = \frac{10 + \{\frac{1}{2}\alpha\mathcal{E} - 2\} Q(2/\sqrt{\alpha\mathcal{E}}) + \{\alpha\mathcal{E} - 8\} Q(2\sqrt{2}/\alpha\mathcal{E}) + \frac{1}{2} \sqrt{\frac{\alpha\mathcal{E}}{\pi}} \{4e^{-\frac{4}{\alpha\mathcal{E}}} + \sqrt{2}e^{-\frac{2}{\alpha\mathcal{E}}}\}}{2 - 2\alpha + \alpha Q(2/\sqrt{\alpha\mathcal{E}}) + 2\alpha Q(2\sqrt{2}/\alpha\mathcal{E})} \quad (38)$$

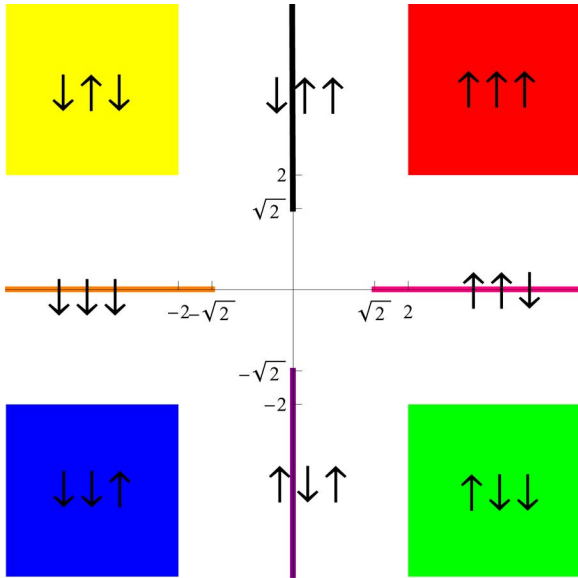


Fig. 6. Octonary stellar relaxation.

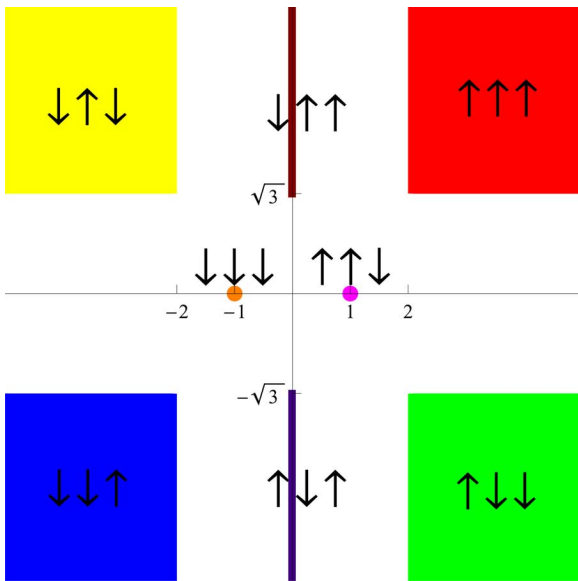


Fig. 7. Octonary triangular relaxation.

and the energy (23) reduces to (40), shown at the bottom of the page.

### VII. INTERFERENCE-FREE TRANSMISSION OVER FINITE SINGULAR CHANNELS

As discussed in Section II-A a vector  $\mathbf{x}$  can be transmitted free of interference as long as it lies in the span of  $\mathbf{E}^{-1}$ . Because the relaxation regions  $\mathcal{A} = \prod_{i=1}^K \mathcal{A}_{s_i}$  proposed in the previous

sections are convex, it is conceivable that the components of a  $K$ -dimensional vector  $\mathbf{x} \in \mathcal{A}$  can be freely tuned in the two-dimensional relaxation regions until the vector is completely contained in the  $N$ -dimensional span of  $\mathbf{E}^{-1}$ . As we shall see, this possibility of overloading is a distinct advantage that convex relaxation schemes offer compared to lattice based schemes such as those proposed in [1], [3], [26]. Another advantage offered by continuous alphabet sets is a greater robustness to channel estimation errors: since information states can be represented by any point within a continuous and finite region, channel estimation errors need not necessarily alter the meaning of the transmitted symbol.

Whether or not interference-free transmission is possible when  $K > N$  boils down to the probability that the precoding space  $\mathcal{A}$  and the span of the matrix  $\mathbf{E}^{-1}$  intersect. To start our analysis we quote the following result by Wendel [27]: the probability that the span of a random  $K \times N$  matrix with i.i.d. real Gaussian entries contains a  $K$ -dimensional vector with all components strictly positive is given by

$$w(K, N) \equiv 2^{1-K} \sum_{\ell=0}^{N-1} \binom{K-1}{\ell}. \quad (41)$$

This result might be extended to show that, if the random entries in the  $K \times N$  matrix are complex Gaussian, then the probability that its span contains a  $K$ -dimensional complex vector with all components in the first quadrant is given by  $w(2K, 2N)$  (see [8, Theorem 1]).

Using the complex extension of Wendel's result and noting that the span of  $\mathbf{H}\mathbf{H}^\dagger$  is the same as that of  $\mathbf{H}$ , in [8] we showed that  $w(2K, 2N)$  is indeed the probability that a vector relaxed in the quaternary space shown in Fig. 2 can be found in the span of  $\mathbf{H}\mathbf{H}^\dagger$ . This is due to the symmetry of the alphabet, the rotational invariance of the span of  $\mathbf{H}\mathbf{H}^\dagger$ , and the radial invariance of its spanning vectors. Then, the probability  $P_Q$  that a quaternary vector relaxed as in Fig. 2 is transmitted free of interference is

$$P_Q(K, N) = w(2K, 2N). \quad (42)$$

The question now is whether the analysis can be extended further and similar results can be found for the relaxed alphabets newly proposed in this paper. Before proceeding, and to get an understanding, let us start by observing that in both the real and complex versions of Wendel's result, the first argument in the function  $f$  corresponds to the number of sign-constrained degrees of freedom the vector exhibits. The second argument indicates the number of dimensions available in the span of the matrix to accommodate such vector.

We shall start by analyzing the probability of interference-free transmission of a  $K$ -dimensional vector  $\mathbf{x}$  using the real binary alphabet shown in Fig. 3. Due to the symmetry of the

$$\mathcal{E} = \frac{18 + \{\alpha\mathcal{E} - 8\}Q(2\sqrt{2/\alpha\mathcal{E}}) + \{\frac{3}{2}\alpha\mathcal{E} - 9\}Q(\sqrt{6/\alpha\mathcal{E}}) + \frac{1}{2}\sqrt{\frac{\alpha\mathcal{E}}{\pi}} \left\{ 4e^{-\frac{4}{\alpha\mathcal{E}}} + 3\sqrt{3}e^{-\frac{3}{\alpha\mathcal{E}}} \right\}}{4 - 4\alpha + 2\alpha Q(2\sqrt{2/\alpha\mathcal{E}}) + 3\alpha Q(\sqrt{6/\alpha\mathcal{E}})} \quad (40)$$

alphabet as well as the unitary invariance of  $\mathbf{H}\mathbf{H}^\dagger$  and the radial invariance of its spanning vectors, we may just consider the probability that a vector with all components strictly positive can be found in the span of  $\mathbf{E}^{-1}$ . The number of sign-constrained degrees of freedom in such a vector is  $K$ . However, symbols in this alphabet might be transmitted using either  $\mathbf{T}_R$  or  $\mathbf{T}_C$  with resulting energy metrics  $\mathbf{E}_R$  or  $\mathbf{E}_C$ , respectively. These two energy metrics have different inverses with different spans, and so they should be treated separately. Because  $\mathbf{E}_R^{-1} = \mathbf{H}_r \mathbf{H}_r^\dagger + \mathbf{H}_i \mathbf{H}_i^\dagger$ , when  $\mathbf{T}_R$  is used the number of degrees of freedom in the span is  $2N$  ( $\mathbf{H}_r$  and  $\mathbf{H}_i$  provide  $N$  real dimensions each). Then the probability  $P_{B1R}$  that a binary vector relaxed in one dimension as shown in Fig. 3 can be transmitted free of interference using  $\mathbf{T}_R$  is

$$P_{B1R}(K, N) = w(K, 2N). \quad (43)$$

However, when  $\mathbf{T}_C$  is used, although the span of  $\mathbf{H}\mathbf{H}^\dagger$  offers in principle  $N$  complex dimensions, these complex degrees of freedom must be constrained down to accommodate  $K$  purely real constraints. Then the total number of real degrees of freedom in the span goes down from  $2N$  to  $2N - K$ . The probability  $P_{B1C}$  that a binary vector relaxed as shown in Fig. 3 can be transmitted free of interference using  $\mathbf{T}_C$  is then

$$P_{B1C}(K, N) = w(K, 2N - K). \quad (44)$$

We now turn our attention to the two-dimensional binary convex relaxation in Fig. 4. Given that the imaginary part is completely unconstrained, the number of sign-constrained degrees of freedom in  $\mathbf{x}$  is, as before,  $K$ . However, precisely because the symbols in  $\mathbf{x}$  need not be one-dimensional the  $2N$  real degrees of freedom available in the complex span of  $\mathbf{H}$  (i.e., the span of  $\mathbf{E}_C^{-1}$ ) are unconstrained. Therefore, the probability  $P_{B2}$  that a binary vector relaxed as shown in Fig. 4 can be transmitted free of interference is

$$P_{B2}(K, N) = w(K, 2N). \quad (45)$$

In the case of the octonary stellar relaxation shown in Fig. 6 each component in  $\mathbf{x}$  can be one or two-dimensional with probability  $1/2$ . Each one-dimensional component has one sign-constrained degree of freedom, and each two-dimensional component has two such degrees of freedom. How many there are of each will condition not only how many constraints there are in  $\mathbf{x}$ , but also how constrained the available degrees of freedom in the span of  $\mathbf{H}$  are. While two-dimensional components do not collapse the rank of the complex span, each one-dimensional component takes away one degree of freedom. Then we might use combinatorics to obtain the probability  $P_{OS}$  that an octonary vector relaxed as shown in Fig. 6 can be transmitted free of interference:

$$P_{OS}(K, N) = \frac{2^K}{2^{2K} - 1} \sum_{q=1}^K \left(\frac{1}{2}\right)^K \binom{K}{q} \times w\left(\frac{q}{K}2K + \frac{K-q}{K}K, 2N - \frac{K-q}{K}K\right). \quad (46)$$

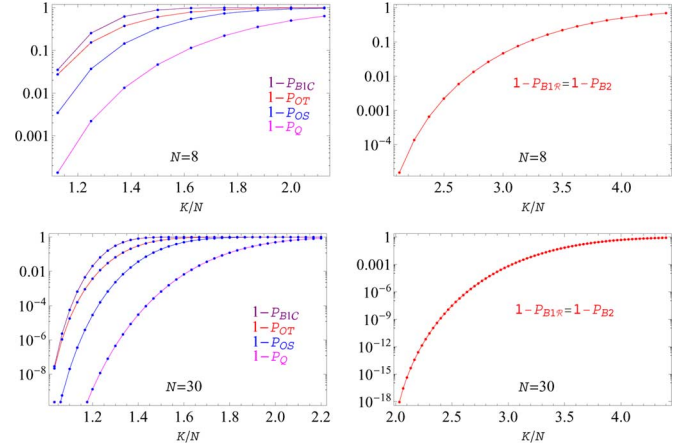


Fig. 8. Probability that convex precoding fails to transmit free of interference versus the ratio of the number of users to the number of transmitting antennas.

Using the octonary triangular relaxation shown in Fig. 7 each component in  $\mathbf{x}$  can be two-dimensional with probability  $1/2$ , one-dimensional with probability  $1/4$ , or a point with probability  $1/4$ . As points have no freedom in any direction, point components in  $\mathbf{x}$  will each collapse two degrees of freedom from the rank of  $\mathbf{H}$ . Treating the one and two-dimensional regions as before, we might obtain the probability  $P_{OT}$  that an octonary vector relaxed as shown in Fig. 7 can be transmitted free of interference:

$$P_{OT}(K, N) = \frac{4^K}{4^K - 3^K - 2^K + 1} \sum_{q=1}^K \sum_{p=1}^{K-q} \left(\frac{1}{2}\right)^q \times \left(\frac{1}{4}\right)^{K-q} \binom{K}{q} \binom{K-q}{p} \times w\left(\frac{q}{K}2K + \frac{K-q-p}{K}K, 2N - \frac{K-q-p}{K}K - \frac{p}{K}2K\right). \quad (47)$$

When it comes to the fully symmetric octonary relaxation space shown in Fig. 5, a similar line of analysis might not be employed due to the nonrectangularity of the precoding regions. Finding the probability that the span of  $\mathbf{H}$  contains a vector relaxed in this space is, to our knowledge, still an open problem.

## VIII. RESULTS AND DISCUSSION

In Fig. 8 we can see a plot of the probability of failing to achieve interference-free transmission. As we can see, depending on the precoding scheme chosen, significant overloads are possible while keeping a relatively small probability of failure, which is perhaps tolerable in systems with subsequent error control coding. As the size of the system increases, the probabilities (42)–(47) tend to become unit step functions of the channel load  $K/N$  such that interference-free transmission is always possible below a certain threshold value.

As the binary relaxation show in Fig. 3 is purely real we might choose to precode it with either  $\mathbf{T}_C$  or  $\mathbf{T}_R$ . When  $\mathbf{T}_C$  is used,

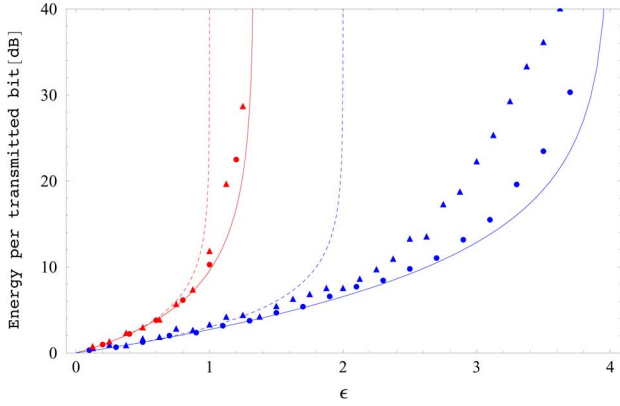


Fig. 9. Energy of vector precoding with the binary real convex relaxation shown in Fig. 3: precoding with  $\mathbf{T}_C$  (red curve) and with  $\mathbf{T}_R$  (blue curve). The blue curve also represents the binary complex convex relaxation shown in Fig. 4 and the quaternary convex relaxation shown in Fig. 2. The triangles and dots alongside the curves are from finite size simulations with  $N = 8$  and  $N = 30$  antennas at the transmitter, respectively, and no failure to achieve interference-free transmission. The discontinuous curves show the energy penalty when SZF precoding is used without alphabet relaxation.

the channel is fully invertible only up to 1 bit/antenna; however, when  $\mathbf{T}_R$  is employed, the channel is fully invertible up to 2 bits/antenna. Also, in Fig. 8 we can see that precoding with  $\mathbf{T}_R$  allows for significant overloads while keeping the probability of failure relatively small.

Precoding the real binary relaxation with  $\mathbf{T}_R$  also results in lower transmission energies than when  $\mathbf{T}_C$  is used. Indeed the use of  $\mathbf{T}_R$  makes optimization over the purely real space perform just as well as over the complex extension shown in Fig. 4, rendering the complexity brought by the search in the additional dimension useless. Furthermore, precoding with  $\mathbf{T}_R$  makes the one-dimensional relaxation for BPSK achieve spectral efficiencies at the same cost as the QPSK relaxation shown in Fig. 2; this means that transmitting 1 bit per user to  $2K$  users has the same cost as transmitting 2 bits per user to  $K$  users. These results are shown in Fig. 9, where the energy per transmitted bit is plotted versus the uncoded spectral efficiency  $\epsilon$ , which is defined as the number of bits per symbol multiplied by the channel load  $K/N$ . Although our analysis pertains to the asymptotic limit, finite size simulations show that these results can be used to approximate finite systems.

When it comes to using the octonary modulation schemes proposed in Section VI, depending on the ratio of transmitting to receiving elements, it might be more advantageous to use the stellar modulation in Section VI-B (S8PSK), or the triangular modulation in Section VI-C (T8PSK). The main advantage that T8PSK presents is that only 6 of the 8 points in the unperturbed constellation are relaxed, which reduces the complexity of the optimization process. Fig. 10 shows the energy per transmitted bit versus  $\epsilon$  attained for all three octonary modulation schemes proposed in Section VI. In the region below 3 bits per transmitting antenna, where all three schemes guarantee interference-free transmission, T8PSK is most appealing given both its lower energy and lower complexity at the implementation stage. As the system gets overloaded T8PSK is outperformed by S8PSK not only in terms of energy penalty, but also,

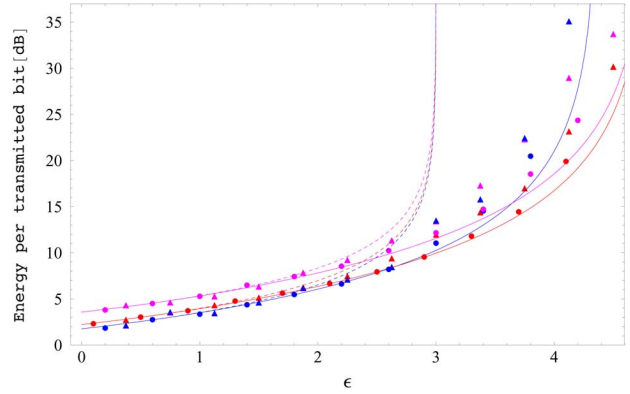


Fig. 10. Energy of vector precoding with the octonary convex relaxation schemes proposed in Section VI: fully symmetric octonary relaxation shown in Fig. 5 (magenta), octonary stellar relaxation shown in Fig. 6 (red curve) and octonary triangular relaxation shown in Fig. 7 (blue curve). The triangles and dots alongside the curves are from finite size simulations with  $N = 8$  and  $N = 30$  antennas at the transmitter, respectively, and no failure to achieve interference-free transmission. The discontinuous curves show the energy penalty when SZF precoding is used without alphabet relaxation.

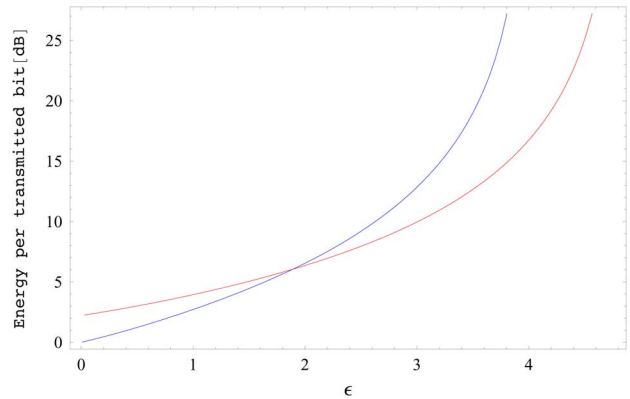


Fig. 11. Red curve: energy of vector precoding with the octonary triangular relaxation shown in Fig. 7. Blue curve: binary real convex relaxation shown in Fig. 3 precoded with  $\mathbf{T}_R$ . The blue curve also equals the performance of the quaternary convex relaxation shown in Fig. 2.

as shown in Fig. 8, in terms of robustness to achieve interference-free transmission.

The ultimate performance measure to compare the different modulation schemes proposed in this work (binary/quaternary/octonary) would be mutual information. This analysis is very challenging and so far has only been done for the quaternary relaxation in Fig. 2 [6], [7]. Another reasonable performance measure to base comparisons upon would be the SNR at the receiver; as this quantity is dominated by the energy penalty at the transmitter (especially at high SNR) we shall, in first approximation, base our comparison upon the energy per transmitted bit. Fig. 11 allows us to compare T8PSK relaxation with the binary and quaternary relaxations shown in Figs. 3 and 2. Uncoded spectral efficiencies of up to  $\sim 1.7$  bits/antenna are attained at a lower cost using either the binary or the quaternary scheme. Depending on the chosen precoding scheme, in the vicinity of 1.7 bits/antenna it costs the same to transmit 1 bit per user to  $K$  users, 2 bits per user to  $K/2$  users, or 3 bits per user to  $K/3$  users.

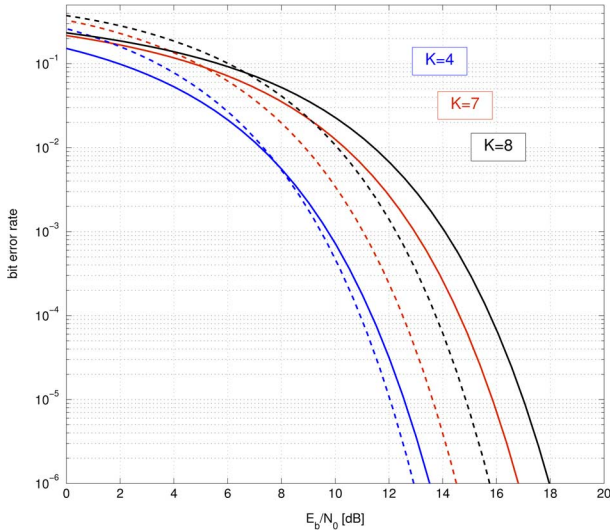


Fig. 12. Bit-error rate versus signal-to-noise ratio for systems with  $N = 8$  transmitting antennas. Solid curves: quaternary convex relaxation in Fig. 2. Dashed curves: two-dimensional quaternary LBVP with four possible lattice points for each of the four information states.

Besides the possibility of overloading, the appeal of using convex precoding schemes (as opposed to lattice-based vector precoding (LBVP) schemes as in [3]) largely resides in the lower complexity of the optimization process. While convex precoding results in a convex optimization problem allowing for efficient polynomial-time algorithms [14], LBVP has a complexity which is exponential in the number of users [13]. In [6], [7] the actual performance of both schemes was compared in terms of mutual information, and it was shown that the relaxation in Fig. 2 is competitive with respect to a two-dimensional quaternary LBVP lattice; indeed the former was shown to outperform the latter at low SNR. The bit-error rate analysis shown in Fig. 12 indicates that a similar conclusion is applicable to finite systems in uncoded communication scenarios.

## IX. CONCLUSION

We have demonstrated that the concept of convex vector precoding is not restricted to QPSK alphabets, but can be extended to both higher and lower order alphabets such as BPSK and 8PSK. For BPSK there exists an optimum way for such a relaxation. Furthermore, this relaxation achieves the same power and bandwidth efficiency as the QPSK relaxation. For 8PSK, there are several competing relaxations that outperform each other depending on the number of users relative to the number of transmit antennas. Furthermore, we show that when it comes to overloading, relaxing onto an area is better than a relaxing onto a line; and relaxations onto a line are better than relaxations onto a set of points.

## APPENDIX A THE R-TRANSFORM

Let  $P_{\mathbf{M}}(x)$  denote the eigenvalue distribution of the matrix  $\mathbf{M}$ . Let

$$m_{\mathbf{M}}(s) = \int \frac{dP_{\mathbf{M}}(x)}{x-s} \quad (48)$$

which is known as the Stieltjes transform. Then, the R-transform of  $P_{\mathbf{M}}(x)$  is

$$R_{\mathbf{M}}(w) = m_{\mathbf{M}}^{\text{inv}}(-w) - \frac{1}{w} \quad (49)$$

with  $m^{\text{inv}}(\cdot)$  denoting the inverse function of  $m(\cdot)$ .

It can be verified that

$$m_{\mathbf{M}^{-1}} \left( \frac{1}{s} \right) = -s(1 + sm_{\mathbf{M}}(s)). \quad (50)$$

Let  $s = m_{\mathbf{M}}^{\text{inv}}(-w)$ . Then, we find

$$m_{\mathbf{M}^{-1}} \left( \frac{1}{m_{\mathbf{M}}^{\text{inv}}(-w)} \right) = -m_{\mathbf{M}}^{\text{inv}}(-w) (1 - wm_{\mathbf{M}}^{\text{inv}}(-w)) \quad (51)$$

and

$$\frac{1}{m_{\mathbf{M}}^{\text{inv}}(-w)} = m_{\mathbf{M}^{-1}}^{\text{inv}}(-m_{\mathbf{M}}^{\text{inv}}(-w) (1 - wm_{\mathbf{M}}^{\text{inv}}(-w))). \quad (52)$$

With (49), we find

$$\frac{1}{R_{\mathbf{M}}(w) + \frac{1}{w}} = R_{\mathbf{M}^{-1}} \left( -wR_{\mathbf{M}}(w) \left( R_{\mathbf{M}}(w) + \frac{1}{w} \right) \right) - \frac{1}{wR_{\mathbf{M}}(w) \left( R_{\mathbf{M}}(w) + \frac{1}{w} \right)} \quad (53)$$

and

$$\frac{1}{R_{\mathbf{M}}(w)} = R_{\mathbf{M}^{-1}}(-R_{\mathbf{M}}(w)(1 + wR_{\mathbf{M}}(w))). \quad (54)$$

It is well known [28, (2.79)] that the R-transform of the limiting spectral measure  $P_{\mathbf{E}_c^{-1}}(x)$  is given by

$$R_{\mathbf{E}_c^{-1}}(w) = \frac{1}{1 - \alpha w}. \quad (55)$$

Letting  $\mathbf{M}^{-1} = \mathbf{E}_c^{-1}$ , we find from (54)

$$R_{\mathbf{E}_c}(w) = 1 + \alpha R_{\mathbf{E}_c}(w) (1 + wR_{\mathbf{E}_c}(w)). \quad (56)$$

Solving (56) for the R-transform yields

$$R_{\mathbf{E}_c}(w) = f_2(w) \quad (57)$$

where  $f_{\tau}(w)$  is defined as

$$f_{\tau}(w) \equiv \frac{\frac{2}{\tau} - \alpha - \sqrt{\left(\frac{2}{\tau} - \alpha\right)^2 - \frac{8}{\tau}\alpha w}}{2\alpha w}. \quad (58)$$

Now, in order to find the R-transform of the spectral measure of  $\mathbf{E}_{\mathcal{R}}$  first we take notice that the matrix  $\mathbf{E}_{\mathcal{R}}^{-1}$  can be written as follows:

$$\mathbf{E}_{\mathcal{R}}^{-1} = \frac{\mathbf{H}_r \mathbf{H}_r^T + \mathbf{H}_i \mathbf{H}_i^T}{N}. \quad (59)$$

Then we note that the R-transform has the following two properties [28], [29]:

$$R_{\mathbf{M}_1+\mathbf{M}_2}(w) = R_{\mathbf{M}_1}(w) + R_{\mathbf{M}_2}(w) \quad (60)$$

$$R_{c\mathbf{M}}(w) = cR_{\mathbf{M}}(cw) \quad \forall c \in \mathbb{C}. \quad (61)$$

Using these two properties we might write the R-transform of (59) as

$$R_{\mathbf{E}_{\mathcal{R}}^{-1}}(w) = \frac{1}{2}R_{\frac{\mathbf{H}_r\mathbf{H}_r^T}{N/2}}\left(\frac{w}{2}\right) + \frac{1}{2}R_{\frac{\mathbf{H}_i\mathbf{H}_i^T}{N/2}}\left(\frac{w}{2}\right). \quad (62)$$

Now recall from Section II that  $\mathbf{H}_r$  and  $\mathbf{H}_i$  are real random matrices containing independent and identically distributed entries with zero mean and variance 1/2. Then both  $(\mathbf{H}_r\mathbf{H}_r^T)/(N/2)$  and  $(\mathbf{H}_i\mathbf{H}_i^T)/(N/2)$  have the same R-transform, which is given by (55) [28, Theorem 2.35], implying that

$$R_{\mathbf{E}_{\mathcal{R}}^{-1}}(w) = \frac{1}{1 - \alpha \frac{w}{2}} \quad (63)$$

which in conjunction with (54) yields that

$$R_{\mathbf{E}_{\mathcal{R}}}(w) = f_1(w). \quad (64)$$

It is now clear by simple substitution how (22) and (23) result from (19) for  $\mathbf{E} = \mathbf{E}_{\mathcal{C}}$  and  $\mathbf{E} = \mathbf{E}_{\mathcal{R}}$ :

$$\begin{aligned} \mathcal{E} &= \frac{\tau}{2} \frac{d}{d\chi} \chi R_{\mathbf{E}}(-\chi) = \frac{q R'_{\mathbf{E}}(-\chi)}{\alpha R_{\mathbf{E}}^2(-\chi)} \\ &= \frac{q}{\tau - \alpha + 2\alpha\chi R_{\mathbf{E}}(-\chi)}. \end{aligned} \quad (65)$$

## APPENDIX B THE REPLICA METHOD

In this Appendix we derive (19)–(21) which are used to obtain the transmitted energy  $\mathcal{E}$  per symbol. The derivation follows along the lines of [5, App. A], but it is extended to allow for purely real matrices such as  $\mathbf{E}_{\mathcal{R}}$ .

Let us start by recalling (18)

$$\mathcal{E} = - \lim_{\beta \rightarrow \infty} \beta^{-1} K^{-1} \ln \sum_{\mathbf{x} \in \mathcal{A} \cap \mathcal{S}} e^{-\beta \mathbf{x}^\dagger \mathbf{E} \mathbf{x}}. \quad (66)$$

As indicated in Section III, the expression in the  $\beta$  limit is a thermodynamic free energy (per microscopic degree of freedom in  $\mathbf{x}$ ) when  $K \rightarrow \infty$ , so, in order to use tools from statistical mechanics and treat the argument in the  $\beta$  limit as a thermodynamic free energy we should write

$$\mathcal{E} = - \lim_{\beta \rightarrow \infty} \lim_{K \rightarrow \infty} \beta^{-1} K^{-1} \ln \sum_{\mathbf{x} \in \mathcal{A} \cap \mathcal{S}} e^{-\beta \mathbf{x}^\dagger \mathbf{E} \mathbf{x}}. \quad (67)$$

As discussed in Section III, the free energy is self-averaging in the thermodynamic limit. Furthermore, the eigenproperties of large random matrices, such as  $\mathbf{E}_{\mathcal{C}}$  and  $\mathbf{E}_{\mathcal{R}}$ , are also postulated to be self-averaging [30]. Hence, we might rewrite (18) as follows:

$$\mathcal{E} = - \lim_{\beta \rightarrow \infty} \overline{\lim_{K \rightarrow \infty} \beta^{-1} K^{-1} \ln \bar{\mathcal{Z}}} \quad (68)$$

where the overbar denotes the configurational average with respect to the matrix  $\mathbf{E}$  (which results from the channel states  $\mathbf{H}$ ), and

$$\bar{\mathcal{Z}} \equiv \sum_{\mathbf{x} \in \mathcal{A} \cap \mathcal{S}_{\mathbf{H}}} e^{-\beta \mathbf{x}^\dagger \mathbf{E} \mathbf{x}}. \quad (69)$$

is referred to as the *partition function*.

Finding the average of the logarithm of a partition function is far from trivial. In order to tackle the problem we employ the somewhat mystifying equality [31, Sec. 6.8]

$$\overline{c \ln \bar{\mathcal{U}}} = \lim_{x \rightarrow 0} \frac{\overline{d\mathcal{U}^x - c}}{x} \quad (70)$$

which for convenience we write as

$$\overline{c \ln \bar{\mathcal{U}}} = \left. \frac{\partial}{\partial n} c \ln \bar{\mathcal{U}}^n \right|_{n=0} \quad (71)$$

where  $c$  is just some constant upon which the probability distribution has no effect.

We might use (71) to rewrite the average in (68) as

$$\overline{\lim_{K \rightarrow \infty} \beta^{-1} K^{-1} \ln \bar{\mathcal{Z}}} = \lim_{n \rightarrow 0} \frac{\partial}{\partial n} \lim_{K \rightarrow \infty} \beta^{-1} K^{-1} \ln \bar{\mathcal{Z}}^n \quad (72)$$

which, moving things around, allows us to write (68) as

$$\mathcal{E} = - \lim_{\beta \rightarrow \infty} \beta^{-1} \lim_{n \rightarrow 0} \frac{\partial}{\partial n} \lim_{K \rightarrow \infty} K^{-1} \ln \bar{\mathcal{Z}}^n. \quad (73)$$

The task is now reformulated in terms of finding the average of a power of the partition function. This is also far from trivial, unless the power is an integer, in which case we are just dealing with moments of  $\bar{\mathcal{Z}}$ . The parameter  $n$  in (73) is, however, a positive real number. In the following we make the key assumption that, although we take  $n$  to be a positive integer, we can nevertheless continually extend the result of the average to  $n = 0$ . This critical assumption together with expression (70), is known as the replica trick, and it is the cornerstone of the replica method, which was developed in statistical physics to analyze magnetic glassy systems. The name *replica* refers to the fact that we are now taking the expectation of the product of  $n$  identical replicas of  $\bar{\mathcal{Z}}$ . We might further rewrite (73) as

$$\mathcal{E} = - \lim_{\beta \rightarrow \infty} \beta^{-1} \lim_{n \rightarrow 0} \frac{\partial}{\partial n} \Xi_n \quad (74)$$

where

$$\begin{aligned} \Xi_n &= \lim_{K \rightarrow \infty} \frac{1}{K} \ln \overline{\prod_{a=1}^n \bar{\mathcal{Z}}_a} \\ &= \lim_{K \rightarrow \infty} \frac{1}{K} \ln \overline{\sum_{\{\mathbf{x}_a \in \mathcal{A} \cap \mathcal{S}_{\mathbf{H}}\}} \exp \left[ \text{tr} \left( -\beta \mathbf{E} \sum_{a=1}^n \mathbf{x}_a \mathbf{x}_a^\dagger \right) \right]} \end{aligned} \quad (75)$$

and the summation notation  $\sum_{\{\mathbf{x}_a \in \mathcal{A} \cap \mathcal{S}_{\mathbf{H}}\}}$  stands for  $\sum_{\mathbf{x}_1 \in \mathcal{A} \cap \mathcal{S}_{\mathbf{H}}} \sum_{\mathbf{x}_2 \in \mathcal{A} \cap \mathcal{S}_{\mathbf{H}}} \cdots \sum_{\mathbf{x}_n \in \mathcal{A} \cap \mathcal{S}_{\mathbf{H}}}$ .

When the random matrix  $\mathbf{E}$  is Hermitian and unitarily invariant the expectation value in (75) can be written in terms of the R-transform  $R_{\mathbf{E}}(w)$  of the eigenvalue distribution of  $\mathbf{E}$  as follows [32]:

$$\Xi_n = \lim_{K \rightarrow \infty} \frac{1}{K} \ln \sum_{\{\mathbf{x}_a \in \mathcal{A} \cap \mathcal{S}_H\}} \exp \left[ -K \sum_{a=1}^n \int_0^{\frac{2}{\tau} \lambda_a} R_{\mathbf{E}}(-w) dw \right] \quad (76)$$

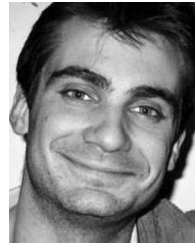
with  $\tau = 1$  when all the entries in  $\mathbf{E}$  are purely real (or purely imaginary) and  $\tau = 2$  when the entries in  $\mathbf{E}$  are neither purely real nor purely imaginary, and with  $\lambda_1, \dots, \lambda_n$  being the eigenvalues of the  $n \times n$  dimensional matrix  $\beta \mathbf{Q}$  whose elements are  $Q_{ab} = K^{-1} \mathbf{x}_a^\dagger \mathbf{x}_b$ .

From this point we follow along the lines of [5, App. A] and obtain expressions (19)–(21).

#### REFERENCES

- [1] R. F. H. Fischer, *Precoding and Signal Shaping for Digital Transmission*. New York: Wiley, 2002.
- [2] C. Windpassinger, R. F. H. Fischer, T. Vencel, and J. B. Huber, "Precoding in multiantenna and multiuser communications," *IEEE Trans. Wireless Commun.*, vol. 3, no. 4, pp. 1305–1316, 2004.
- [3] B. M. Hochwald, C. Peel, and A. Swindlehurst, "A vector-perturbation technique for near-capacity multiantenna multiuser communication—Part II: Perturbation," *IEEE Trans. Commun.*, vol. 53, no. 3, pp. 537–544, Mar. 2005.
- [4] M. Joham, W. Utschick, and J. A. Nossek, "Linear transmit processing in MIMO communication systems," *IEEE Trans. Signal Process.*, vol. 53, no. 8, pp. 537–544, Aug. 2005.
- [5] R. R. Müller, D. Guo, and A. Moustakas, "Vector precoding for wireless MIMO systems and its replica analysis," *IEEE J. Sel. Areas Commun.*, vol. 26, pp. 530–540, Apr. 2008.
- [6] B. M. Zaidel, R. R. Müller, R. de Miguel, and A. L. Moustakas, "On spectral efficiency of vector precoding for Gaussian MIMO broadcast channels," presented at the IEEE Int. Symp. Spread Spectrum Techniques Applications (ISSSTA), Bologna, Italy, Aug. 2008.
- [7] B. M. Zaidel, R. R. Müller, R. de Miguel, and A. L. Moustakas, "On replica symmetry breaking in vector precoding for the Gaussian MIMO broadcast channel," presented at the Proc. 46th Annu. Allerton Conf. Communication, Control, Computing, Monticello, IL, Sep. 2008.
- [8] R. de Miguel, V. Gardasevic, R. R. Müller, and F. F. Knudsen, "On overloaded vector precoding for single-user MIMO channels," *IEEE Trans. Wireless Comm.*, Jan. 2009, accepted for publication.
- [9] R. Schober, W. H. Gerstacker, and L. Lampe, "On suboptimum receivers for DS-CDMA with BPSK modulation," *Signal Process.*, vol. 85, pp. 1149–1163, 2005.
- [10] B. R. Vojčić and W. M. Jang, "Transmitter precoding in synchronous multiuser communications," *IEEE Trans. Commun.*, vol. 46, pp. 1346–1355, Oct. 1998.
- [11] C. B. Peel, B. M. Hochwald, and A. L. Swindlehurst, "A vector-perturbation technique for near-capacity multiantenna multiuser communication—Part I: Channel inversion and regularization," *IEEE Trans. Commun.*, vol. 53, pp. 195–202, Jan. 2005.
- [12] D. A. Schmidt, M. Joham, and W. Utschick, "Minimum mean square error vector precoding," *Eur. Trans. Telecommun.*, vol. 19, pp. 219–231, 2008.
- [13] J. Jalden and B. Ottersten, "On the complexity of sphere decoding in digital communications," *IEEE Trans. Signal Process.*, vol. 53, no. 4, pp. 1474–1484, Apr. 2005.
- [14] S. P. Boyd and L. Vandenberghe, *Convex Optimization*. Cambridge, U.K.: Cambridge Univ. Press, 2004.
- [15] R. V. de Miguel de Juan, "On the analysis and design of wireless communication systems using tools from statistical physics," Doctoral dissertation, Norwegian Uni. Sci. and Technol., Trondheim, Norway, 2009, 2009:7.
- [16] W. Greiner, H. Stocker, and L. Neise, *Thermodynamics and Statistical Mechanics (Classical Theoretical Physics)*. New York: Springer, 1995.
- [17] D. Sherrington and S. Kirkpatrick, "Solvable model of a spin glass," *Phys. Rev. Lett.*, vol. 35, 1975.
- [18] T. Tanaka, "A statistical mechanics approach to large-system analysis of CDMA multiuser detectors," *IEEE Trans. Inf. Theory*, vol. 48, pp. 2888–2910, Nov. 2002.
- [19] A. L. Moustakas, S. H. Simon, and A. M. Sengupta, "MIMO capacity through correlated channels in the presence of correlated interferers and noise: A (not so) large n analysis," *IEEE Trans. Inf. Theory*, vol. 49, no. 10, pp. 2545–2561, Oct. 2003.

- [20] R. R. Müller and W. H. Gerstacker, "On the capacity loss due to separation of detection and decoding," *IEEE Trans. Inf. Theory*, vol. 50, pp. 1769–1778, Aug. 2004.
- [21] D. Guo and S. Verdú, "Randomly spread CDMA: Asymptotics via statistical physics," *IEEE Trans. Inf. Theory*, vol. 51, no. 6, pp. 1983–2010, Jun. 2005.
- [22] Y. Kabashima and D. Saad, "Statistical mechanics of error-correcting codes," *Europhys. Lett.*, vol. 45, 1999.
- [23] A. Montanari and N. Sourlas, "The statistical mechanics of turbo codes," *Eur. Phys. J. B*, vol. 18, pp. 107–119, 2000.
- [24] V. Dotsenko, *Introduction to the Replica Theory of Disordered Statistical Systems*. Cambridge, U.K.: Cambridge Univ. Press, 2001.
- [25] H. Nishimori, *Statistical Physics of Spin Glasses and Information Processing (International Series of Monographs on Physics)*. Oxford, U.K.: Oxford Univ. Press, 2001, vol. 111.
- [26] M. Taherzadeh, A. Mobasher, and A. K. Khandani, "Communication over MIMO broadcast channels using lattice-basis reduction," *IEEE Trans. Inf. Theory*, vol. 53, no. 12, pp. 4567–4582, Dec. 2007.
- [27] J. G. Wendel, "A problem in geometric probability," *Math. Scand.*, vol. 11, pp. 109–111, 1962.
- [28] A. M. Tulino and S. Verdú, "Random matrix theory and wireless communications," *Found. Trends Commun. Inf. Theory*, vol. 1, Jun. 2004.
- [29] D. V. Voiculescu, K. J. Dykema, and A. Nica, *Free Random Variables*. Providence, RI: Amer. Math. Soc., 1992.
- [30] M. L. Mehta, *Random Matrices*, 2nd ed. New York: Academic, 1991.
- [31] G. H. Hardy, J. E. Littlewood, and G. Pólya, *Inequalities*. Cambridge, U.K.: Cambridge Univ. Press, 1934.
- [32] A. Guionnet and M. Maïda, "A Fourier view on the R-transform and related asymptotics of spherical integrals," *J. Function. Anal.*, vol. 222, pp. 435–490, 2005.



**Rodrigo de Miguel** was born in Madrid, Spain, in 1978. He received the B.S. degree in physics from the University of Puget Sound, Tacoma, WA, and the Ph.D. degree for his research at the interphase between statistical physics and wireless communications from Norwegian University of Science and Technology (NTNU), Trondheim, Norway, in 2001 and 2009, respectively.

In 2006, he was a Visiting Scholar in the Department of Physics, Bar Ilan University, Tel Aviv, Israel.

In 2005, he joined the Department of Electronics and Telecommunications at NTNU. In 2003, he was awarded a Marie Curie Fellowship by the European Commission to analyze some physical factors contributing to the inefficiency of fuel cells. He was granted a Chemical Physics Fellowship by the Institute for Physical Science and Technology, University of Maryland, College Park, where he passed the Ph.D. qualifying examination in 2002. At the University of Puget Sound, he was inducted as a member of Sigma Pi Sigma, The Physics Honor Society (American Institute of Physics).



**Ralf R. Müller** (S'96–M'03–SM'05) was born in Schwabach, Germany, in 1970. He received the Dipl. Ing. and Dr. Ing. degrees with distinction from the University of Erlangen-Nuremberg, Bavaria, Germany, in 1996 and 1999, respectively.

Since 2005, he has been a Full Professor in the Department of Electronics and Telecommunications, Norwegian University of Science and Technology (NTNU), Trondheim, Norway. From 2000 to 2004, he directed a research group at Vienna Telecommunications Research Center, Vienna, Austria, and

taught as an Adjunct Professor at the Vienna University of Technology. He held visiting appointments at Princeton University, Princeton, NJ; Institute Eurecom, France; University of Melbourne, Australia; University of Oulu, Finland; National University of Singapore; Babes-Bolyai University, Cluj-Napoca, Romania; and Kyoto University, Japan.

Dr. Müller was presented awards for his dissertation, "Power and bandwidth efficiency of multiuser systems with random spreading," by the Vodafone Foundation for Mobile Communications and the German Information Technology Society (ITG). Moreover, he received the ITG award for the paper, "A random matrix model for communication via antenna arrays," as well as the Philipp-Reis Award (jointly with Robert Fischer). He received the Leonard G. Abraham Prize (jointly with Sergio Verdú) for the paper, "Design and analysis of low-complexity interference mitigation on vector channels" from the IEEE Communications Society. He served as an associate editor for the IEEE TRANSACTIONS ON INFORMATION THEORY from 2003 to 2006.